Effects of halloysite content on the thermo-mechanical performances of composite bioplastics

Lorenzo Lisuzzo[a], Giuseppe Cavallaro[a,b,*] Stefana Milioto[a,b], Giuseppe Lazzara[a,b]

[a]Dipartimento di Fisica e Chimica, Università degli Studi di Palermo, Viale delle Scienze, pad. 17, 90128 Palermo, Italy. *giuseppe.cavallaro@unipa.it*

[b]Consorzio Interuniversitario Nazionale per la Scienza e Tecnologia dei Materiali, INSTM, Via G. Giusti, 9, I-50121 Firenze, Italy

Keywords: Halloysite, bioplastics, biopolymer, nanocomposites, DMA, TGA

Abstract

The aim of this study is the design and preparation of Mater-Bi/halloysite nanocomposite materials that could be employed as bioplastics alternative to the petroleum derived products. The biocomposite materials at variable halloysite content (from 0 to 30 wt%) were prepared by using the solvent casting method. We investigated the mechanical behaviour and the thermal properties of the prepared nanocomposites in order to estimate their suitability as biocompatible packaging materials. The thermo-mechanical characteristics were correlated to the nanocomposites' morphologies, which were studied by Scanning Electron Microscopy (SEM). As a general result, the physico-chemical performances of Mater-Bi were improved by the presence of small amounts of nanotubes, which evidenced a homogenous distribution in the polymer matrix. The strongest enhancements of the thermal stability and tensile properties were achieved for Mater-Bi/halloysite 10 wt%. A further addition of nanotubes determined the worsening of both thermal stability and mechanical behaviour.

The attained knowledge represents the starting step for the development of packaging films composed by Mater-Bi and halloysite nanotubes.

1. Introduction

Environmental issues, e.g. pollution and climate change, are the most urgent challenges that science must tackle in the medium period. The need to exploit and strengthen all the possibilities that green chemistry offers is compelling. Therefore, scientists and researchers are making great efforts with the aim to provide new green tools to the society, thus ensuring a more respectful development model. Herein, the use of petroleum derived materials must be restricted due to their harmful impact on the ecosystem and their non-biocompatibility. In the most recent years, new bio-derived materials have been designed and studied with the purpose to replace traditional plactics. Hence, the term "bioplastics" derived from the need to develop novel eco-sustainable systems without waiving some important physico-chemical properties.

Biopolymers represent a profitable alternative for the design of new eco-friendly functional materials being completely green, eco-sustainable and non-toxic (Liu et al., 2012; Gorrasi, 2015; Biddeci et al., 2016; Rebitski et al., 2018). They can display some different features in relation with the natural source where the raw matter is extracted and used during the preparation procedure (Tharanathan, 2003; Mensitieri et al., 2011). The biopolymers charge is one of the most important feature that affect their suitability in numerous applications (Bertolino et al., 2016). Among the sustainable polymers, chitosan is positively charged, alginate and pectin are negatively charged, starch and cellulose are neutral. It is also important to consider the different hydrophilic/hydrophobic behaviours of such species that, in light of these reasons, offer a wide range of choice to material scientists and engineers.

Nevertheless, some limitations to the use of pure biopolymers still exist and they are related to the mechanical, thermal or gas barrier properties (Gorrasi et al., 2014; Lvov et al., 2016; Sharma et al., 2018). In order to overcome these constraints, the most promising bioplastics are prepared through the combination of both organic moieties and some inorganic fillers, such as clay nanoparticles (Dziadkowiec et al., 2017; Almeida et al., 2019; Rebitski et al., 2019). Nanoclays are attracting the

attention of the scientific community due to their peculiar features in terms of chemistry, morphology, aspect ratio and charge (Peyne et al., 2017; Djellali et al., 2019; Lisuzzo et al., 2019b). Among the clay nanoparticles, halloysite (Hal) is a 1:1 aluminosilicate that can be found in nature, whose main property is its distinctive hollow tubular shape combined with its eco-compatibility, no-toxicity and low cost (Joo et al., 2013; Zhang, 2017). Each halloysite nanotube is composed by a layer of tetrahedral siloxanes and a layer of octahedral aluminols forming a sheet that rolls up, thus creating two chemically different surfaces (Joussein et al., 2005). The outer surface (composed by Si-O-Si groups) is negatively charged and the inner one (composed by Al-OH groups) is positively charged in the 2-8 pH range (Lazzara et al., 2018). Moreover, halloysite nanotubes show a high aspect ratio, since the inner diameter is about 10-20 nm, the outer diameter is 50-70 nm and the length is 1-2 μm. Within this, it should be noted that the polydispersion degree in sizes is strongly affected by the specific geological source of halloysite (Cavallaro et al., 2018a). Recently, halloysite nanotube-based functional materials have received increasing attention as evidenced by research articles (Tan et al., 2014; Zeng et al., 2019) and reviews (Yuan et al., 2015; Papoulis, 2019). Halloysite is a promising nanoclay in numerous applications, including drug delivery (Viseras et al., 2008; Aguzzi et al., 2013; Dzamukova et al., 2015), catalysis (Liu et al., 2018; Sadjadi et al., 2018) and remediation (Berthonneau et al., 2015; Nyankson et al., 2015; Panchal et al., 2018; Deng et al., 2019; Wei et al., 2019) . There are many examples proving the importance of halloysite in addition to ecocompatible polymers as starting building blocks for the preparation of novel green materials with specific biomedical and technological functionalities (Silva et al., 2014; Naumenko et al., 2016; Qin et al., 2016; Liu et al., 2017; Zhou et al., 2017; Ali and Ahmed, 2018; Zhao et al., 2018; Suner et al., 2019). For instance, biocomposites with a multilayered morphology based on a layer of halloysite sandwiched between two layers of chitosan were designed for medical or fire retardancy applications (Bertolino et al., 2018). Literature reports the formation of a chitosan film with embedded clay nanotubes used for the preparation of alginate covered tablets, which exhibited pH controlled drug delivery capacity (Lisuzzo et al., 2019a). Bioplastics were prepared

105 by filling halloysite into the pectin matrix for food packaging applications (Makaremi et al., 2017)
106 and by combining lisozyme loaded nanotubes and poly (ε-caprolactone) (PCL) for the preparation
107 of antimicrobial packaging membrane (Bugatti et al., 2017). Moreover, bionanocomposites based
108 were obtained by the halloysite addition into cellulose and chitosan for the delivery of curcumin or
109 tissue engineering applications, respectively (Liu et al., 2013; Huang et al., 2017).
110 In our previous work (Cavallaro et al., 2018), we investigated the effect of different nanoclays
111 (sepiolite, halloysite, laponite and kaolinite) in the mechanical properties of Mater-Bi polymer
112 based nanocomposites with a fixed polymer/nanofiller ratio. The results showed that halloysite is
113 the most promising nanoclay for the preparation of bioplastics that present Mater-Bi as polymeric
114 matrix. Here, we studied the influence of the halloysite content on both the mechanical and thermal
115 features of the bionanocomposites in order to determine an effective protocol for the development
116 of Mater-Bi/halloysite hybrid films with proper characteristics for packaging purposes.

117

118 **2. Materials and methods**

119 2.1 *Materials*

120 Halloysite (Hal) was supplied as a "processed product" by Imerys from their Matauri Bay
121 operation. Mater-Bi is a Novamont product (Novara, Italy) and 1,2-Dichloroethane was purchased
122 by Sigma-Aldrich.

123 2.2 *Preparation of the nanocomposites*

124 The nanocomposites based on halloysite nanotubes and Mater-Bi were prepared by solvent casting
125 method. Firstly, the biopolymer (2 wt %) was solubilized in 1,2-Dichloroethane and Hal was added
126 as dry powder to the solution at different concentrations, from 0 to 30% w/w. Thereafter, each
127 mixture was magnetically stirred overnight at 25 °C and poured down into glass Petri dishes in
128 order to evaporate the solvent, thus obtaining different nanocomposite films, which were stored in a
129 desiccator at 25 °C.

130 2.3 *Methods*

131 2.3.1. *Dynamic Mechanical Analysis*

132 A DMA Q800 instrument (TA Instruments) was used in order to study the tensile properties of the
133 Mater-Bi/Hal nanocomposites. In particular, the films were cut into rectangular shaped portions
134 (10.00×5.00×0.20 mm^3) and the measurements were performed with a stress ramp of 1 MPa min^{-1}
135 at 25.0 ± 0.5 ◦C. The analysis of the stress vs strain curves allowed us to determine the Young
136 modulus (*Ym*), the tensile strenght (σ_r) and the percentage of elongation at break ($\varepsilon_{\%}$). The
137 integration of each curve provided the stored energy (*E*) for each film due to the mechanical stress
138 until the breaking point.

139

140 2.3.2. *Thermogravimetry*

141 Thermogravimetric analysis (TGA) was performed using a Q5000 IR apparatus (TA Instruments)
142 under the nitrogen flow of 25 $cm^3\ min^{-1}$ for the sample and 10 $cm^3\ min^{-1}$ for the balance. The
143 calibration was carried out by means of Curie temperature of standards (nickel, cobalt and their
144 alloys) as reported in literature (Blanco et al., 2014, 2017). Each sample, whose mass was ca. 5 mg,
145 was heated from room temperature to 750 °C with a rate of 20 °C min^{-1}. TGA allowed to study the
146 thermal degradation of Mater-Bi/Hal nanocomposites and to investigate any effects on the thermal
147 stability of these materials.

148

149 2.3.3. *Scanning Electron Microscopy*

150 The morphological features of the nanocomposites were studied by scanning electron microscopy,
151 which was conducted using a ESEM FEI QUANTA 200F microscope. In order to avoid any
152 charging under electron beam, each sample was coated with gold in argon by means of an Edwards
153 Sputter Coater S150A before the analysis. The measurements were carried out in high-vacuum

mode ($< 6 \times 10^{-4}$ Pa) for simultaneous secondary electrons. The energy of the beam was 20 kV, while the working distance was set at 10 mm.

2.3.4. *Fourier transform infrared (FTIR) spectroscopy*

Fourier transform infrared (FTIR) measurements were performed at room temperature through a Frontier FTIR spectrometer (PerkinElmer). The spectra were recorded using 64 scans in the range between 4000 and 450 cm^{-1}, while the spectral resolution was set at 2 cm^{-1}. The experiments were conducted on KBr pellets with a low content (< 2 wt%) of milled sample.

3. Results and discussion

3.1. *Mechanical properties of Mater-Bi/Halloysite composite films*

Some examples of stress vs. strain curves for Mater-Bi and Mater-Bi/halloysite films are presented in Figure 1.

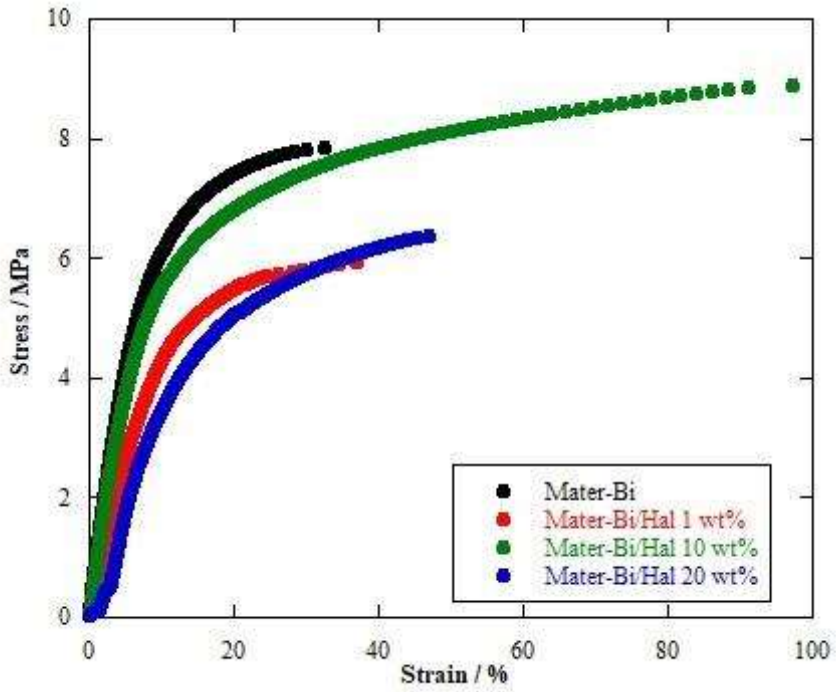

Figure 1. Stress vs. strain curves for pure Mater-Bi and Mater-Bi/Halloysite films as a function of the nanoclay content.

171 The stress vs. strain curves (Figure 1) showed that all the prepared samples are elastic at first, since
172 the strain increases linearly with the stress, and they convert into plastic materials when the yelding
173 point is reached, thus the deformation becomes irreversible. Moreover, it was observed that the
174 strain at break is much higher for the Mater-Bi/Hal 10 wt% nanocomposite in comparison with the
175 other samples. The dependence of the elongation at break on the nanofiller content is shown in
176 Figure 2.

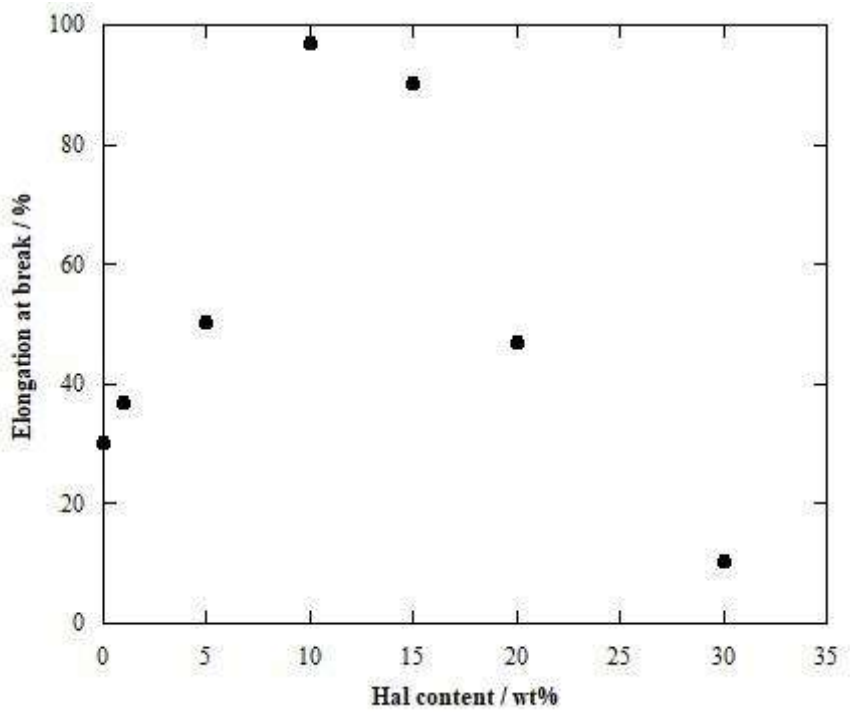

177

178 **Figure 2.** Elongation at break for Mater-Bi/Halloysite composite films as a function of the nanoclay
179 content. The relative error is 2%.

180

181 It is clearly observed that the concentration of inorganic nanotubes deeply influences the ultimate
182 elongation of Mater-Bi based films (Figure 2). In particular, we detected that the percentage of
183 ultimate elongation is 30 and 100% for the pure Mater-Bi film and Mater-Bi/Hal 10 wt%,
184 respectively The further addition of nanotubes decreased the elongation at break up to ca. 10% for
185 the composite material with the largest Hal content (30 wt%). According to the literature (Tang and
186 Alavi, 2012; Cavallaro et al., 2013), the reduction of the maximum elongation can be explained by

considering the nanotubes/Mater-Bi interactions, which avoid the sliding of the polymer chains. Similar effects were observed for the stored energy of the films during the tensile experiments (Figure 3).

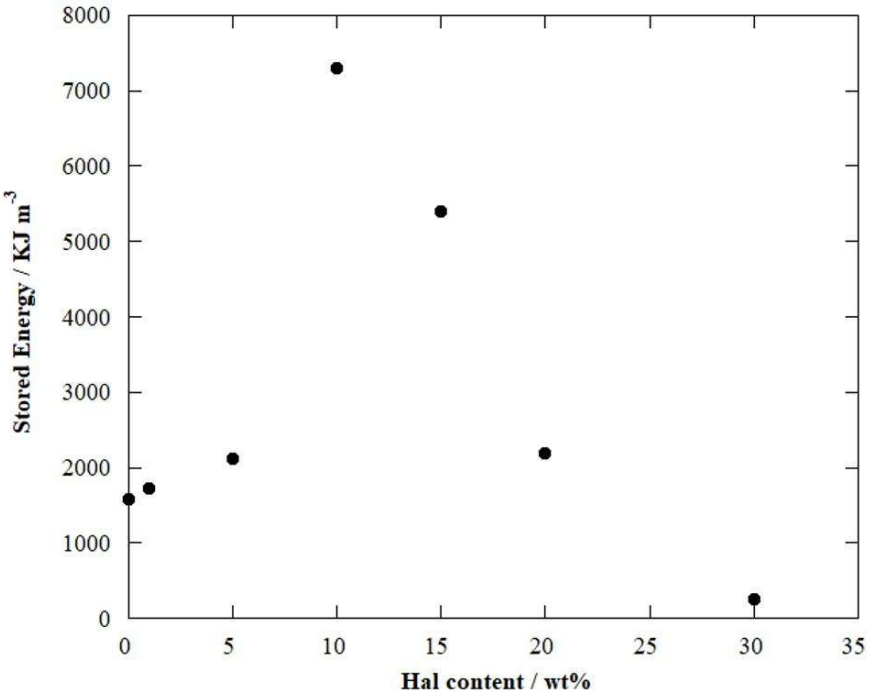

Fig. 3. Stored energy up to breaking for Mater-Bi/Halloysite composite films as a function of the nanoclays content. The relative error is 2%.

Specifically, we determined that the film based on pristine Mater-Bi possess a stored energy of 1718 kJ m^{-3}. This value was significantly enhanced in the composite with Hal concentration of 10 wt% (ca. 7300 kJ m^{-3}), while the Mater-Bi/Hal 30 wt% exhibited a much lower stored energy (254 kJ m^{-3}). These observations are in good agreement with the data of both stress at break and Young modulus (see Supporting Information).

202 3.2. *Thermal properties and structure*

203 Thermogravimetric analysis was aimed to study the thermal stability and the degradation properties
204 of the Mater-Bi/Hal nanocomposite film. As examples, Figure 4 reports the thermogravimetric
205 curves for both pure Mater-Bi and Mater-Bi/Hal_10 wt% materials.

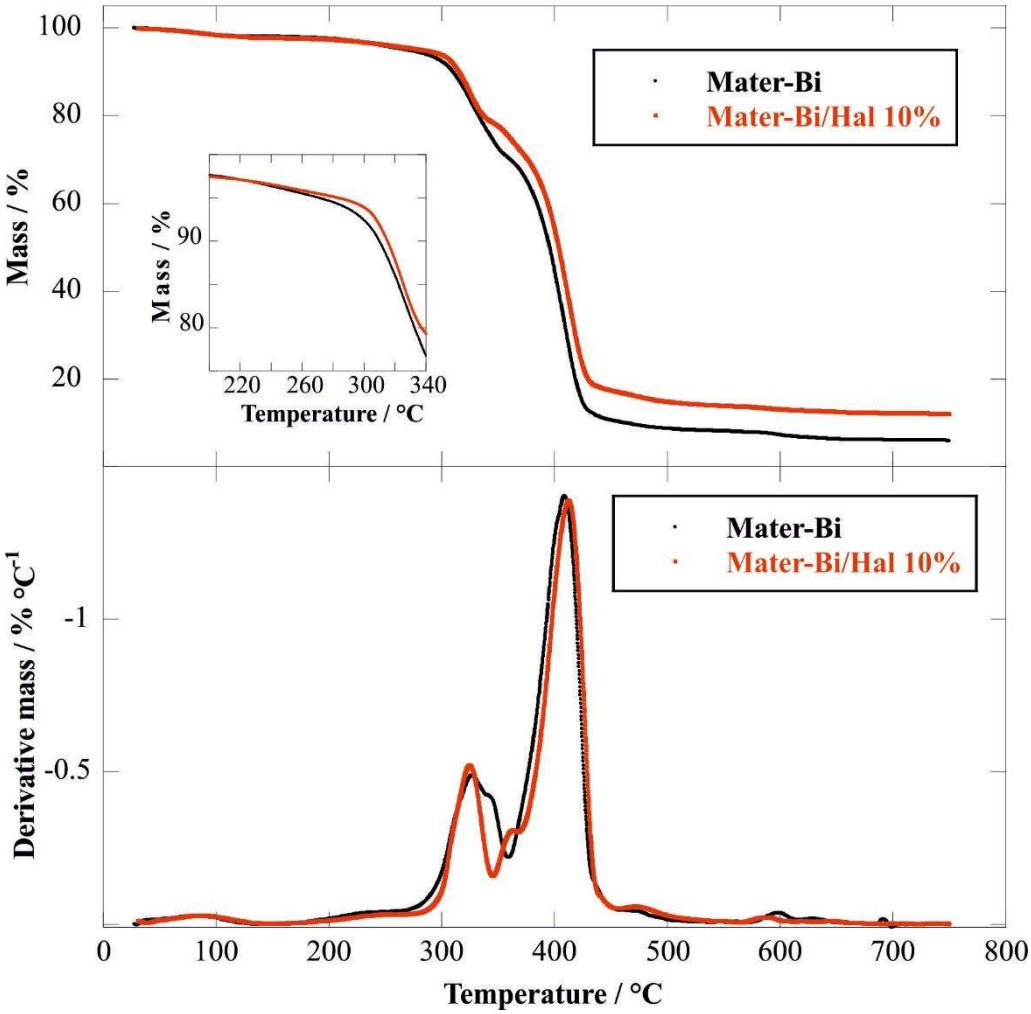

206

207 **Figure 4.** Thermogravimetric (up) and differential thermogravimetric (bottom) curves for Mater-Bi
208 and Mater-Bi/Hal 10 wt% materials. The inset shows the thermogravimetric curves for for Mater-Bi
209 and Mater-Bi/Hal 10 wt% within the temperature range between 200 and 340 °C.

210

211 Compared to pristine Mater-Bi, the nanocomposite presents a larger residual mass at high
212 temperature as a consequence of the presence of the inorganic nanotubes (Figure 4). In this regards,
213 the residual masses at 700 °C for all the investigated materials are presented in Supporting
214 Information. These results evidenced that the nanocomposites with higher Hal contents possess

larger residual masses at 700 °C. All the investigated materials showed a mass loss in the temperature range between 25 and 150 °C that can be attributed to the moisture content of the bioplastics. Both Mater-Bi and Mater-Bi/Hal 10 wt% nanocomposite exhibited two different degradation steps in the 300-400°C range as highlighted by the corresponding differential thermogravimetric curves (Figure 4). In order to explore the effect of halloysite on the thermal stability of Mater-Bi, we determined the onset temperatures from the analysis of the thermogravimetric curves. The onset temperature refers to the initial decomposition of Mater-Bi. Namely, it represents the temperature where the polymer starts to decompose. The onset temperature is obtained by the intersection of a line tangent to the baseline the with a line tangent to the inflection point of the thermogravimetric curve.

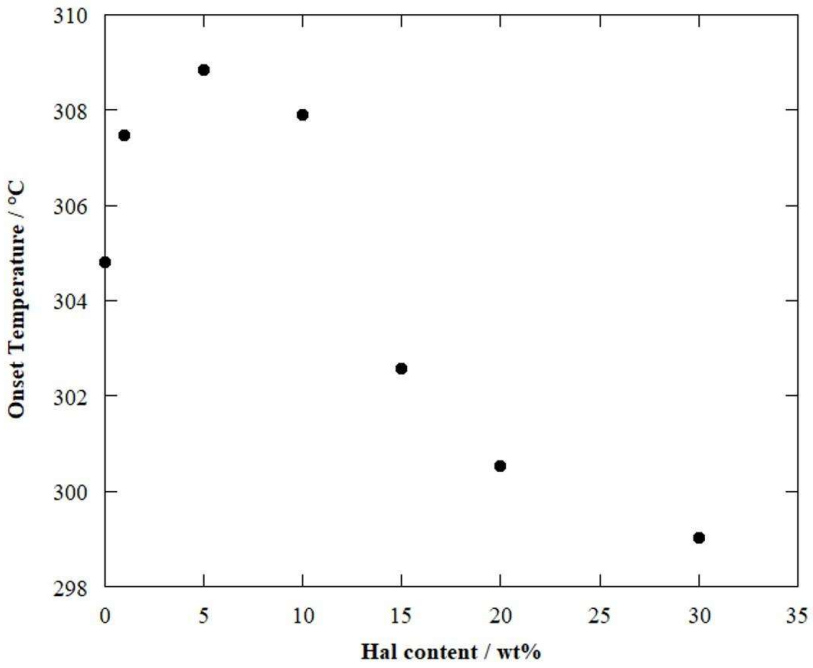

Figure 5. Onset temperature values for pure Mater-Bi and Mater-Bi/Halloysite composite films as a function of the nanoclay content. The relative error is 2%.

Similarly to the tensile properties, the presence of small amounts of halloysite generated a slight improvement of the Mater-Bi thermal stability (Figure 5). In particular, the nanocomposite with Hal content of 10 wt% showed an enhancement of ca. 4 °C for the onset temperature with respect to that

of pristine Mater-Bi. The slight thermal stabilization effect induced by the presence of small amounts of halloysite can be observed by the comparison of the thermogravimetric curves for Mater-Bi and Mater-Bi/Hal 10 wt% within the temperature range between 200 and 340 °C (see inset in Figure 4). Larger filler contents (> 10 wt%) induced a worsening of the polymer thermal stability as evidenced by the decrease of the onset temperature (Figure 5). Similar trends are reported for the degradation temperatures estimated by the maxima of the DTG peaks (see Supporting Information).These effects might be related to the peculiar morphological characteristics of the nanocomposites that can be influenced by their specific composition. Based on thermogravimetric results, the nanotubes should be uniformly dispersed in the polymeric matrix for the composite materials with Hal ≤ 10 wt%. This hypothesis was supported by SEM images (Figure 6), which showed that Mater-Bi/Hal 10 wt% presents the nanotubes randomly dispersed in its surface.

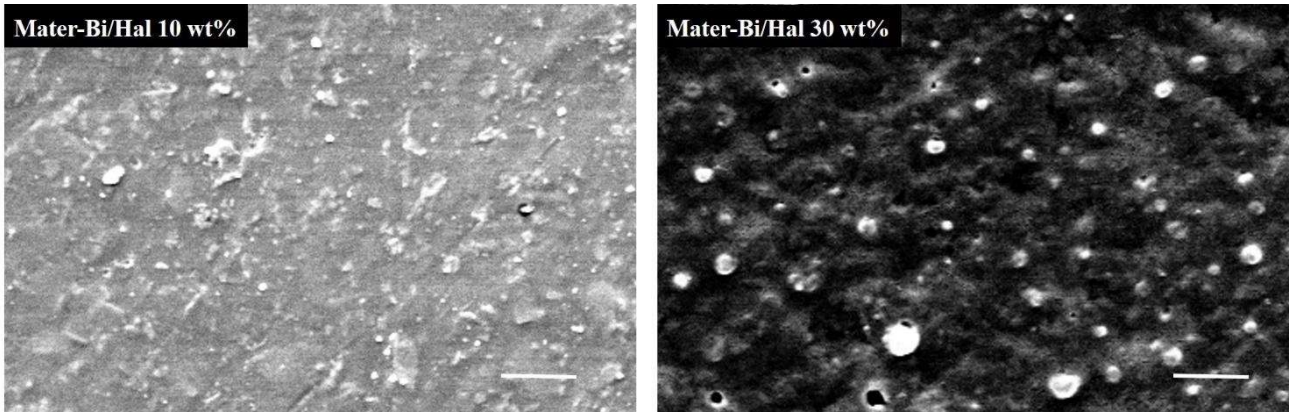

Figure 6. Scanning Electron Microscopy image of the Mater-Bi/Hal nanocomposites at variable composition. The scale bar is 10 μm.

As reported in literature (Du et al., 2006, 2010; Makaremi et al., 2017), the homogenous distribution of inorganic fillers within polymer can cause an enhancement of the thermal stability as a consequence of the barrier effect towards the volatile products of the polymer degradation. Furthermore, the encapsulation process within the Hal cavity can contribute to the improvement of the Mater-Bi resistance to the thermal degradation. On the other hand, the decrease of the onset

253 temperature at larger Hal contents could be an indication of the phase separation between polymer
254 and nanotubes, which are not more able to create a barrier towards the volatile products of the
255 Mater-Bi degradation. In this regards, it is reported that nanocomposites with a large Hal content
256 exhibit a lower thermal stability compared to the corresponding pure polymers because of their
257 layered structure (Cavallaro et al., 2011) and/or formation of nanotubes aggregates within the
258 matrix (Cavallaro et al., 2013). As evidenced in Figure 6, Mater-Bi/Hal 30 wt% presents a rough
259 surface with several clusters and holes indicating that the nanotubes are not homogeneously
260 dispersed in the polymeric matrix. Accordingly, both the thermal and mechanical properties of
261 Mater-Bi were worsened by the addition of a large amounts of halloysite nanotubes. The nature of
262 interactions between Mater-Bi and halloysite nanotubes in the nanocomposites was investigated by
263 FTIR spectroscopy. Figure 7 shows the FTIR spectra for Mater-Bi and Mater-Bi with variable Hal
264 content (10 and 30 wt%).

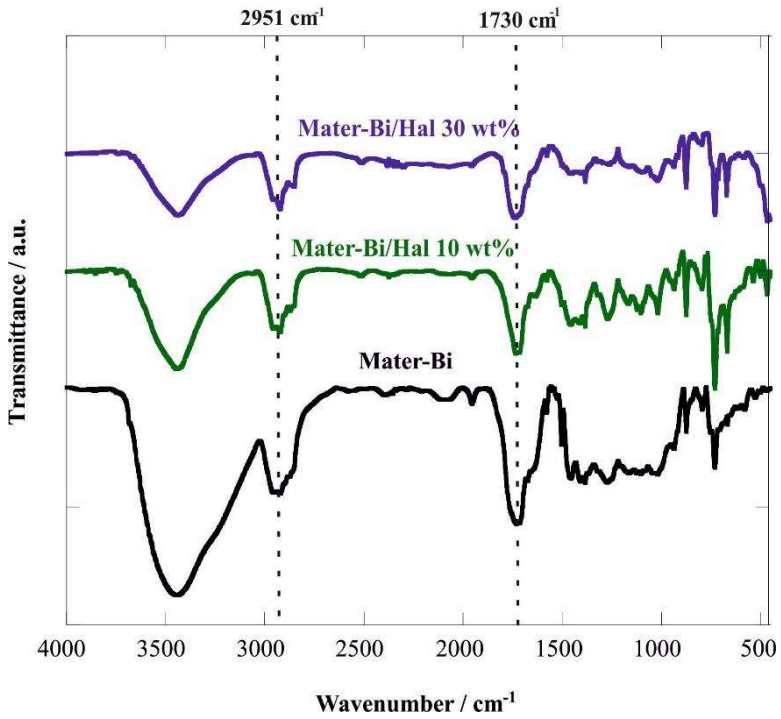

265

266 **Figure 7.** Fourier Transform Infrared spectra for Mater-Bi, Mater-Bi/Hal 10 wt% and Mater-Bi/Hal
267 30 wt% materials.

We observed that the characteristic FTIR signals of Mater-Bi are not influenced by the presence of halloysite. In particular, we focused on the peaks centered at 2951 and 1730 cm^{-1}, which are related to C-H aliphatic stretching and C=O stretching vibration of polyester, respectively (Cataldi et al., 2015). Both signals did not show neither shifting nor splitting phenomena in the Mater-Bi/Hal nanocomposites highlighting that the polymer structure was not altered by the addition of the nanotubes. Based on FTIR spectra, we can state that Mater-Bi is physically adsorbed onto halloysite surfaces ruling out the presence of covalent bonds between matrix and filler.

4. Conclusions

We successfully prepared a novel biohybrid material based on Mater-Bi and halloysite nanotubes by using the casting method from 1,2-Dichloroethane. The effect of the halloysite content on the tensile and thermal properties of the nanocomposites was extensively investigated by Dynamic Mechanical Analysis (DMA) and Thermogravimetry (TGA), respectively.

As a general result, we detected that the presence of small amounts (≤ 10 wt%) of nanotubes confers improved thermo-mechanical performances with respect to those of Mater-Bi. Compared to the pure biopolymer, Mater-Bi/Hal 10 wt% composite exhibited improvements of ca. 320 and 230% for the ultimate elongation and the stored energy at the breaking point, respectively. Opposite results were detected for nanocomposites with Hal concentrations larger than 10 wt%. As example, the stored energy at break evidenced a decrease of ca. 85% in the nanocomposite with halloysite content of 30 wt%. Similar effects were observed for the elastic modulus and the stress at breaking point. As concerns the thermal behavior, we observed that the thermal stability of Mater-Bi/halloysite nanocomposites slightly depends on their specific filler content. The addition of nanotubes generated enhancements (up to 4 °C) of the polymer degradation temperature for halloysite contents lower than 10 wt%. Oppositely, a thermal destabilization of Mater-Bi was detected for nanocomposites with halloysite concentrations larger than 10 wt%. In particular,

293 Mater-Bi/halloysite 30 wt% evidenced a slight decrease (ca. 5 °C) of the polymer degradation
294 temperature with respect to that of pure Mater-Bi that can be attributed to the formation of
295 halloysite clusters within the matrix. According to both TGA and DMA data, we can conclude that
296 the most promising performances were achieved for Mater-Bi/halloysite 10 wt% composite film,
297 which might be considered as a suitable biomaterial for packaging applications.
298
299 **5. Supporting Information**
300 Young modulus as a function of halloysite content for Mater-Bi/Hal nanocomposites. Stress at
301 breaking point as a function of halloysite content for Mater-Bi/Hal nanocomposites. Polymer
302 degradation temperature (first DTG peak) as a function of halloysite content for Mater-Bi/Hal
303 nanocomposites. Polymer degradation temperature (second DTG peak) as a function of halloysite
304 content for Mater-Bi/Hal nanocomposites. Thermogravimetric curves and thermogravimetric
305 parameters (residual mass at 700 °C and mass loss in temperature range between 25 and 150 °C) of
306 all investigated Mater-Bi based materials.
307
308 **6. Acknowledgments**
309 The work was financially supported by Progetto di ricerca e sviluppo "AGM for CuHe"
310 (ARS01_00697) and University of Palermo. The authors have no conflicts of interest to declare.
311
312 **7. References**
313 Aguzzi, C., Viseras, C., Cerezo, P., Salcedo, I., Sánchez-Espejo, R., Valenzuela, C., 2013. Release
314 kinetics of 5-aminosalicylic acid from halloysite. Colloids and Surfaces B: Biointerfaces
315 105, 75–80. https://doi.org/10.1016/j.colsurfb.2012.12.041
316 Ali, A., Ahmed, S., 2018. A review on chitosan and its nanocomposites in drug delivery. Int. J.
317 Biol. Macromol. 109, 273–286. https://doi.org/10.1016/j.ijbiomac.2017.12.078
318 Almeida, J.A., Oliveira, A.S., Rigoti, E., Neto, J.C.D., de Alcântara, A.C.S., Pergher, S.B.C., 2019.
319 Design of solid foams for flame retardant based on bionanocomposites systems. App Clay
320 Sci 180, 105173. https://doi.org/10.1016/j.clay.2019.105173
321 Berthonneau, J., Grauby, O., Jeannin, C., Chaudanson, D., Joussein, E., Baronnet, A., 2015. Native
322 Morphology of Hydrated Spheroidal Halloysite Observed by Environmental Transmission

Electron Microscopy. Clay Clay Miner 63, 368–377. https://doi.org/10.1346/CCMN.2015.0630503
Bertolino, V., Cavallaro, G., Lazzara, G., Merli, M., Milioto, S., Parisi, F., Sciascia, L., 2016. Effect of the biopolymer charge and the nanoclay morphology on nanocomposite materials. Industrial and Engineering Chemistry Research 55, 7373–7380. https://doi.org/10.1021/acs.iecr.6b01816
Bertolino, V., Cavallaro, G., Lazzara, G., Milioto, S., Parisi, F., 2018. Halloysite nanotubes sandwiched between chitosan layers: novel bionanocomposites with multilayer structures. New J. Chem. 42, 8384–8390. https://doi.org/10.1039/C8NJ01161C
Biddeci, G., Cavallaro, G., Di Blasi, F., Lazzara, G., Massaro, M., Milioto, S., Parisi, F., Riela, S., Spinelli, G., 2016. Halloysite nanotubes loaded with peppermint essential oil as filler for functional biopolymer film. Carbohydrate Polymers 152, 548–557. https://doi.org/10.1016/j.carbpol.2016.07.041
Blanco, I., Abate, L., Bottino, F.A., Bottino, P., 2014. Thermal behaviour of a series of novel aliphatic bridged polyhedral oligomeric silsesquioxanes (POSSs)/polystyrene (PS) nanocomposites: The influence of the bridge length on the resistance to thermal degradation. Polym. Degrad. Stab. 102, 132–137. https://doi.org/10.1016/j.polymdegradstab.2014.01.029
Blanco, I., Cicala, G., Latteri, A., Saccullo, G., El-Sabbagh, A.M.M., Ziegmann, G., 2017. Thermal characterization of a series of lignin-based polypropylene blends. J Therm Anal Calorim 127, 147–153. https://doi.org/10.1007/s10973-016-5596-2
Bugatti, V., Viscusi, G., Naddeo, C., Gorrasi, G., 2017. Nanocomposites Based on PCL and Halloysite Nanotubes Filled with Lysozyme: Effect of Draw Ratio on the Physical Properties and Release Analysis. Nanomaterials 7. https://doi.org/10.3390/nano7080213
Cataldi, P., Bayer, I.S., Bonaccorso, F., Pellegrini, V., Athanassiou, A., Cingolani, R., 2015. Foldable Conductive Cellulose Fiber Networks Modified by Graphene Nanoplatelet-Bio-Based Composites. Adv Electron Mater 1, 1500224. https://doi.org/10.1002/aelm.201500224
Cavallaro, G., Chiappisi, L., Pasbakhsh, P., Gradzielski, M., Lazzara, G., 2018a. A structural comparison of halloysite nanotubes of different origin by Small-Angle Neutron Scattering (SANS) and Electric Birefringence. App Clay Sci 160, 71–80. https://doi.org/10.1016/j.clay.2017.12.044
Cavallaro, G., Donato, D.I., Lazzara, G., Milioto, S., 2011. Films of Halloysite Nanotubes Sandwiched between Two Layers of Biopolymer: From the Morphology to the Dielectric, Thermal, Transparency, and Wettability Properties. J. Phys. Chem. C 115, 20491–20498. https://doi.org/10.1021/jp207261r
Cavallaro, G., Lazzara, G., Lisuzzo, L., Milioto, S., Parisi, F., 2018b. Filling of Mater-Bi with Nanoclays to Enhance the Biofilm Rigidity. J Funct Biomater 9. https://doi.org/10.3390/jfb9040060
Cavallaro, G., Lazzara, G., Milioto, S., 2013. Sustainable nanocomposites based on halloysite nanotubes and pectin/polyethylene glycol blend. Polymer Degradation and Stability 98, 2529–2536. https://doi.org/10.1016/j.polymdegradstab.2013.09.012
Deng, L., Yuan, P., Liu, D., Du, P., Zhou, J., Wei, Y., Song, Y., Liu, Y., 2019. Effects of calcination and acid treatment on improving benzene adsorption performance of halloysite. App Clay Sci 181, 105240. https://doi.org/10.1016/j.clay.2019.105240
Djellali, M., Aranda, P., Ruiz-Hitzky, E., 2019. Silica-layered double hydroxide nanoarchitectured materials. App Clay Sci 171, 65–73. https://doi.org/10.1016/j.clay.2019.02.004
Du, M., Guo, B., Jia, D., 2010. Newly emerging applications of halloysite nanotubes: a review. Polym. Int. 59, 574–582.
Du, M., Guo, B., Jia, D., 2006. Thermal stability and flame retardant effects of halloysite nanotubes on poly(propylene). Eur. Polym. J. 42, 1362–1369. https://doi.org/doi: 10.1016/j.eurpolymj.2005.12.006

Dzamukova, M.R., Naumenko, E.A., Lvov, Y.M., Fakhrullin, R.F., 2015. Enzyme-activated intracellular drug delivery with tubule clay nanoformulation. Sci. Rep. 5, 10560.
Dziadkowiec, J., Mansa, R., Quintela, A., Rocha, F., Detellier, C., 2017. Preparation, characterization and application in controlled release of Ibuprofen-loaded Guar Gum/Montmorillonite Bionanocomposites. App Clay Sci 135, 52–63. https://doi.org/10.1016/j.clay.2016.09.003
Gorrasi, G., 2015. Dispersion of halloysite loaded with natural antimicrobials into pectins: Characterization and controlled release analysis. Carbohydr. Polym. 127, 47–53. https://doi.org/10.1016/j.carbpol.2015.03.050
Gorrasi, G., Pantani, R., Murariu, M., Dubois, P., 2014. PLA/Halloysite Nanocomposite Films: Water Vapor Barrier Properties and Specific Key Characteristics. Macromol. Mater. Eng. 299, 104–115. https://doi.org/10.1002/mame.201200424
Huang, B., Liu, M., Zhou, C., 2017. Cellulose–halloysite nanotube composite hydrogels for curcumin delivery. Cellulose 24, 2861–2875. https://doi.org/10.1007/s10570-017-1316-8
Joo, Y., Sim, J.H., Jeon, Y., Lee, S.U., Sohn, D., 2013. Opening and blocking the inner-pores of halloysite. Chem. Commun. 49, 4519–4521. https://doi.org/10.1039/C3CC40465J
Joussein, E., Petit, S., Churchman, G.J., Theng, B., Righi, D., Delvaux, B., 2005. Halloysite clay minerals — a review. Clay Miner 40, 383–426.
Lazzara, G., Cavallaro, G., Panchal, A., Fakhrullin, R., Stavitskaya, A., Vinokurov, V., Lvov, Y., 2018. An assembly of organic-inorganic composites using halloysite clay nanotubes. Curr. Opin. Colloid Interface Sci. 35, 42–50. https://doi.org/10.1016/j.cocis.2018.01.002
Lisuzzo, L., Cavallaro, G., Milioto, S., Lazzara, G., 2019a. Layered composite based on halloysite and natural polymers: a carrier for the pH controlled release of drugs. New J. Chem. 43, 10887–10893. https://doi.org/10.1039/C9NJ02565K
Lisuzzo, L., Cavallaro, G., Pasbakhsh, P., Milioto, S., Lazzara, G., 2019b. Why does vacuum drive to the loading of halloysite nanotubes? The key role of water confinement. Journal of Colloid and Interface Science 547, 361–369. https://doi.org/10.1016/j.jcis.2019.04.012
Liu, F., Bai, L., Zhang, H., Song, H., Hu, L., Wu, Y., Ba, X., 2017. Smart H2O2-Responsive Drug Delivery System Made by Halloysite Nanotubes and Carbohydrate Polymers. ACS Appl. Mater. Interfaces 9, 31626–31633. https://doi.org/10.1021/acsami.7b10867
Liu, M., Wu, C., Jiao, Y., Xiong, S., Zhou, C., 2013. Chitosan-halloysite nanotubes nanocomposite scaffolds for tissue engineering. J. Mater. Chem. B 1, 2078–2089. https://doi.org/10.1039/C3TB20084A
Liu, M., Zhang, Y., Wu, C., Xiong, S., Zhou, C., 2012. Chitosan/halloysite nanotubes bionanocomposites: Structure, mechanical properties and biocompatibility. Int. J. Biol. Macromol. 51, 566–575. https://doi.org/10.1016/j.ijbiomac.2012.06.022
Liu, Y., Guan, H., Zhang, J., Zhao, Y., Yang, J.-H., Zhang, B., 2018. Polydopamine-coated halloysite nanotubes supported AgPd nanoalloy: An efficient catalyst for hydrolysis of ammonia borane. Int. J. Hydrogen Energ. 43, 2754–2762. https://doi.org/10.1016/j.ijhydene.2017.12.105
Lvov, Y., Wang, W., Zhang, L., Fakhrullin, R., 2016. Halloysite Clay Nanotubes for Loading and Sustained Release of Functional Compounds. Adv Mater 28, 1227–1250. https://doi.org/10.1002/adma.201502341
Makaremi, M., Pasbakhsh, P., Cavallaro, G., Lazzara, G., Aw, Y.K., Lee, S.M., Milioto, S., 2017. Effect of Morphology and Size of Halloysite Nanotubes on Functional Pectin Bionanocomposites for Food Packaging Applications. ACS Appl. Mater. Inter 9, 17476–17488. https://doi.org/10.1021/acsami.7b04297
Mensitieri, G., Di Maio, E., Buonocore, G.G., Nedi, I., Oliviero, M., Sansone, L., Iannace, S., 2011. Processing and shelf life issues of selected food packaging materials and structures from renewable resources. Trends Food Sci. Tech. 22, 72–80. https://doi.org/10.1016/j.tifs.2010.10.001

Naumenko, E.A., Guryanov, I.D., Yendluri, R., Lvov, Y.M., Fakhrullin, R.F., 2016. Clay nanotube–biopolymer composite scaffolds for tissue engineering. Nanoscale 8, 7257–7271. https://doi.org/10.1039/C6NR00641H

Nyankson, E., Olasehinde, O., John, V.T., Gupta, R.B., 2015. Surfactant-Loaded Halloysite Clay Nanotube Dispersants for Crude Oil Spill Remediation. Industrial & Engineering Chemistry Research 54, 9328–9341. https://doi.org/10.1021/acs.iecr.5b02032

Panchal, A., Swientoniewski, L.T., Omarova, M., Yu, T., Zhang, D., Blake, D.A., John, V., Lvov, Y.M., 2018. Bacterial proliferation on clay nanotube Pickering emulsions for oil spill bioremediation. Colloids Surf. B Biointerfaces 164, 27–33. https://doi.org/10.1016/j.colsurfb.2018.01.021

Papoulis, D., 2019. Halloysite based nanocomposites and photocatalysis: A Review. Appl. Clay Sci. 168, 164–174. https://doi.org/10.1016/j.clay.2018.11.009

Peyne, J., Gautron, J., Doudeau, J., Joussein, E., Rossignol, S., 2017. Influence of silicate solution preparation on geomaterials based on brick clay materials. Journal of Non-Crystalline Solids 471, 110–119. https://doi.org/10.1016/j.jnoncrysol.2017.05.017

Qin, L., Zhao, Y., Liu, J., Hou, J., Zhang, Y., Wang, J., Zhu, J., Zhang, B., Lvov, Y., Van der Bruggen, B., 2016. Oriented Clay Nanotube Membrane Assembled on Microporous Polymeric Substrates. ACS Appl. Mater. Interfaces 8, 34914–34923. https://doi.org/10.1021/acsami.6b12858

Rebitski, E.P., Alcântara, A.C.S., Darder, M., Cansian, R.L., Gómez-Hortigüela, L., Pergher, S.B.C., 2018. Functional Carboxymethylcellulose/Zein Bionanocomposite Films Based on Neomycin Supported on Sepiolite or Montmorillonite Clays. ACS Omega 3, 13538–13550. https://doi.org/10.1021/acsomega.8b01026

Rebitski, E.P., Souza, G.P., Santana, S.A.A., Pergher, S.B.C., Alcântara, A.C.S., 2019. Bionanocomposites based on cationic and anionic layered clays as controlled release devices of amoxicillin. App Clay Sci 173, 35–45. https://doi.org/10.1016/j.clay.2019.02.024

Sadjadi, S., Heravi, M.M., Malmir, M., 2018. Pd@HNTs-CDNS-g-C3N4: A novel heterogeneous catalyst for promoting ligand and copper-free Sonogashira and Heck coupling reactions, benefits from halloysite and cyclodextrin chemistry and g-C3N4 contribution to suppress Pd leaching. Carbohydr. Polym. 186, 25–34. https://doi.org/10.1016/j.carbpol.2018.01.023

Sharma, B., Malik, P., Jain, P., 2018. Biopolymer reinforced nanocomposites: A comprehensive review. Mater Today Commun 16, 353–363. https://doi.org/10.1016/j.mtcomm.2018.07.004

Silva, R.D., Pasbakhsh, P., Goh, K.L., Chai, S.-P., Chen, J., 2014. Synthesis and characterisation of poly (lactic acid)/halloysite bionanocomposite films. Journal of Composite Materials 48, 3705–3717.

Suner, S.S., Demirci, S., Yetiskin, B., Fakhrullin, R., Naumenko, E., Okay, O., Ayyala, R.S., Sahiner, N., 2019. Cryogel composites based on hyaluronic acid and halloysite nanotubes as scaffold for tissue engineering. Int. J. Biol. Macromol. 130, 627–635. https://doi.org/10.1016/j.ijbiomac.2019.03.025

Tan, D., Yuan, P., Annabi-Bergaya, F., Liu, D., Wang, L., Liu, H., He, H., 2014. Loading and in vitro release of ibuprofen in tubular halloysite. Appl. Clay Sci. 96, 50–55. https://doi.org/10.1016/j.clay.2014.01.018

Tang, X., Alavi, S., 2012. Structure and Physical Properties of Starch/Poly Vinyl Alcohol/Laponite RD Nanocomposite Films. J. Agric. Food Chem. 60, 1954–1962. https://doi.org/10.1021/jf2024962

Tharanathan, R.N., 2003. Biodegradable films and composite coatings: past, present and future. Trends Food Sci. Tech. 14, 71–78. https://doi.org/doi: DOI: 10.1016/S0924-2244(02)00280-7

Viseras, M.T., Aguzzi, C., Cerezo, P., Viseras, C., Valenzuela, C., 2008. Equilibrium and kinetics of 5-aminosalicylic acid adsorption by halloysite. Micropor. Mesopor. Mat. 108, 112–116. https://doi.org/10.1016/j.micromeso.2007.03.033

476 Wei, Y., Yuan, P., Liu, D., Losic, D., Tan, D., Chen, F., Liu, H., Zhou, J., Du, P., Song, Y., 2019.
477 Activation of natural halloysite nanotubes by introducing lanthanum oxycarbonate
478 nanoparticles via co-calcination for outstanding phosphate removal. Chem. Commun. 55,
479 2110–2113. https://doi.org/10.1039/C8CC10314C
480 Yuan, P., Tan, D., Annabi-Bergaya, F., 2015. Properties and applications of halloysite nanotubes:
481 recent research advances and future prospects. Appl. Clay Sci. 112–113, 75–93.
482 https://doi.org/10.1016/j.clay.2015.05.001
483 Zhang, H., 2017. Selective modification of inner surface of halloysite nanotubes: a review.
484 Nanotechnol Rev 6, 573. https://doi.org/10.1515/ntrev-2017-0163
485 Zhao, Y., Kong, W., Jin, Z., Fu, Y., Wang, W., Zhang, Y., Liu, J., Zhang, B., 2018. Storing solar
486 energy within Ag-Paraffin@Halloysite microspheres as a novel self-heating catalyst.
487 Applied Energy 222, 180–188. https://doi.org/10.1016/j.apenergy.2018.04.013
488 Zeng, X., Zhong, B., Jia, Z., Zhang, Q., Chen, Y., Jia, D., 2019. Halloysite nanotubes as
489 nanocarriers for plant herbicide and its controlled release in biodegradable polymers
490 composite film. Appl Clay Sci 171, 20–28. https://doi.org/10.1016/j.clay.2019.01.021
491 Zhou, X., Zhang, Q., Wang, R., Guo, B., Lvov, Y., Hu, G.-H., Zhang, L., 2017. Preparation and
492 performance of bio-based carboxylic elastomer/halloysite nanotubes nanocomposites with
493 strong interfacial interaction. Compos. Part A-Appl. S. 102, 253–262.
494 https://doi.org/10.1016/j.compositesa.2017.08.013
495

496

497

498

499